Biochimica et Biophysica Acta, 510 (1978) 264—269

BBA 78055

PHYTOHEMAGGLUTININ AND TRANSMEMBRANE PROTEINS IN AGGLUTINATED SHEEP ERYTHROCYTE GHOST MEMBRANES

W. LESSLAUER

Department of Pathology, Kantonsspital, Basel (Switzerland)

(Received October 31st, 1977)

Summary

Oriented and periodically stacked sheep erythrocyte ghost membrane specimens were prepared by agglutination of the ghosts with phytohemagglutinin M and sedimentation, and were studied by X-ray diffraction. The spatial orientation of the planes of the membranes in the diffracting stack was determined from the lamellar reflections of the periodic stacking. Equatorial diffraction at $(10.5\ \text{Å})^{-1}$ and a $(1.5\ \text{Å})^{-1}$ reflection were recorded which correlate with side-to-side packed transmembrane α-helices in the agglutinated membrane. A broad $(4.6\ \text{Å})^{-1}$ ring with strong equatorial accentuation and broad maxima at about $(2.2\ \text{Å})^{-1}$ and $(1.2\ \text{Å})^{-1}$ were observed which are attributed to the hydrocarbon chain arrangement in lipid phases of the agglutinated ghost membrane.

Introduction

Oriented and periodically stacked specimens of sheep erythrocyte membranes are obtained by agglutination of isolated ghosts with phytohemagglutinin M and sedimentation; from X-ray diffraction the lamellar period in the fully hydrated stacks is about 180 Å and contains two asymmetric membranes [1]. In addition to lamellar reflections, X-ray difraction from membrane proteins and lipid phases is recorded. The diffraction from membrane proteins in the agglutinated ghost pellets differs from what is known of the native, non-agglutinated ghost membrane [2,3]. The agglutinated ghost pellets are composite structures of membranes, phytohemagglutinin and serum protein molecules [1]; structural rearrangements might occur in the erythrocyte membrane upon agglutination [4,5].

Materials and Methods

Agglutinated ghost pellets were prepared from red blood cells of Grison mountain sheep essentially as described previously [1]. Buffer solutions used

were Tris · HCl (10^{-2} M, pH 7.4) with 10% inactivated sheep serum or 1.0 mg purified sheep serum albumin/ml; they were made isotonic with added NaCl. Sodium dodecyl sulphate-polyacrylamide gel electrophoresis with 1.5 mm thick slabs and a discontinuous buffer system was carried out according to Maizel [6]. X-Ray diffraction was done as described previously [1].

Results

X-Ray diffraction from agglutinated sheep erythrocyte ghost membranes shows (1) a series of meridional reflections due to the lamellar stacking of the membranes (if the direction of the lamellar diffraction is defined as meridian), (2) a broad (10.5 Å)$^{-1}$ ring, (3) a broad (4.6 Å)$^{-1}$ ring, and (4) a broad ring at about (3.3 Å)$^{-1}$ [1]. In other exposures, (2.2 Å)$^{-1}$, (1.5 Å)$^{-1}$ and (1.2 Å)$^{-1}$ reflections are recorded.

The biochemical conditions of preparations were such that no differences between agglutinated and native ghosts were detected by gel electrophoresis, except that the agglutinin and albumin became part of the membrane specimens.

(10.5 Å)$^{-1}$ and (1.5 Å)$^{-1}$ diffraction. The intensity of the (10.5 Å)$^{-1}$ ring from agglutinated ghosts is higher at the equator than at the meridian (Fig. 1). The radially integrated intensity of the ring as a function of the off-meridional angle is plotted in Fig. 2. The (10.5 Å)$^{-1}$ ring is well resolved at the equator; its baseline in the densitometer traces was determined, therefore, by drawing first a smooth curve through the minima on either side of

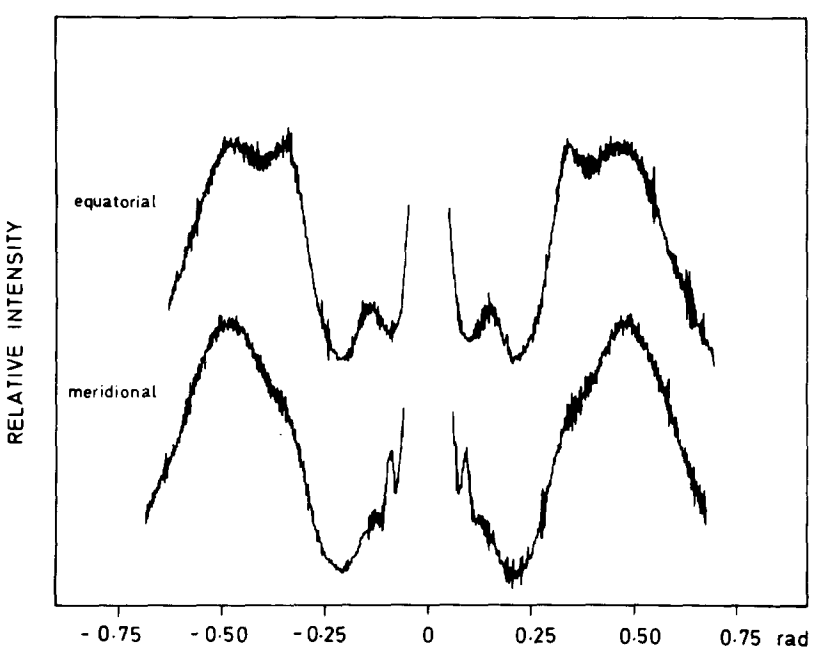

Fig. 1. Densitometer traces of the (10.5 Å)$^{-1}$, (4.6 Å)$^{-1}$ and (3.3 Å)$^{-1}$ diffraction. Equatorial and meridional traces of the same film are shown. In the meridional trace (bottom) a strong lamellar reflection is resolved also. (Diffraction angle, 2θ in radians)

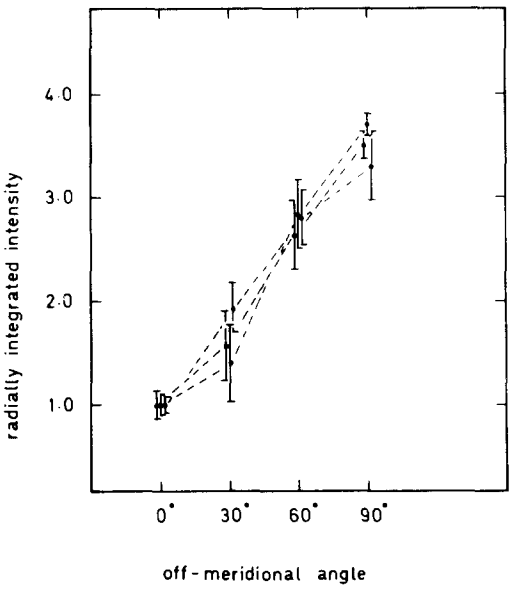

Fig. 2. Radially integrated intensity of the $(10.5\ \text{Å})^{-1}$ ring as a function of the angle from meridian to equator. Means and standard deviations of three independent experiments are given. See text for determination of baseline.

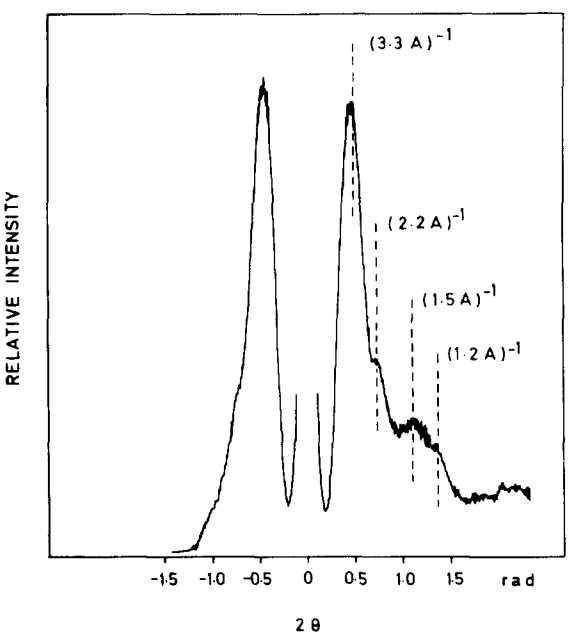

Fig. 3. Densitometer trace of the $(2.2\ \text{Å})^{-1}$, $(1.5\ \text{Å})^{-1}$ and $(1.2\ \text{Å})^{-1}$ reflections and the symmetric $(3.3\ \text{Å})^{-1}$ water band. The specimen was tilted by about 31° from the orientation for optimal lamellar diffraction and oscillated by ±5° during the exposure. The pattern was recorded with a cylindrical film cassette. (Diffraction angle 2θ in radians)

the ring in the equatorial trace. This baseline was then transferred onto intermediate and meridional traces by superimposing the maxima of the $(3.3\ \text{Å})^{-1}$ water ring. This results in a falsely low baseline at the meridian, where $(10.5\ \text{Å})^{-1}$ ring and lamellar reflections overlap (Fig. 1). No corrections for this error in the baseline or for membrane disorientation were applied in Fig. 2. The ratio of the equatorial and meridional intensities of the $(10.5\ \text{Å})^{-1}$ ring in Fig. 2, therefore, must be regarded as a lower limit.

In order to record the $(1.5\ \text{Å})^{-1}$ reflection, the spatial orientation of the membranes in the specimen was first determined by visual inspection and short exposures of the lamellar reflections [1]. The specimen was then tilted from the position of optimal lamellar diffraction by an angle ϕ = arc sin $(1.54/2 \cdot 1.5) \simeq 31°$ around an axis parallel to the planes of the membranes and perpendicular to the beam. During the exposure the specimen was oscillated by $\pm 5°$ around this axis in the new position. Patterns were recorded with a cylindrical film cassette. The specimen was placed in the centre and with the planes of the membranes parallel to the symmetry axis of the cassette. With this geometry, 1.5 Å spacings perpendicular to the membranes are brought onto the sphere of reflection and can be recorded. A densitometer trace of such a diffraction pattern (Fig. 3) demonstrates that a meridional $(1.5\ \text{Å})^{-1}$ reflection is recorded at the diffraction angle $2\,\theta_{(1.5\text{Å})} = +2$ arc sin $(\lambda/2d)$, but not at the angle $-2\,\theta_{(1.5\text{Å})}$.

$(4.6\ \text{Å})^{-1}$, $(2.2\ \text{Å})^{-1}$ and $(1.2\ \text{Å})^{-1}$ diffraction. The $(4.6\ \text{Å})^{-1}$ ring from the agglutinated ghost pellets when recorded with a plane film cassette shows strong equatorial accentuation (Figs. 1 and 4). The baseline of the $(4.6\ \text{Å})^{-1}$ ring for the determination of the radially integrated intensity in Fig. 4 was obtained by a linear interpolation of the minima on either side of the ring

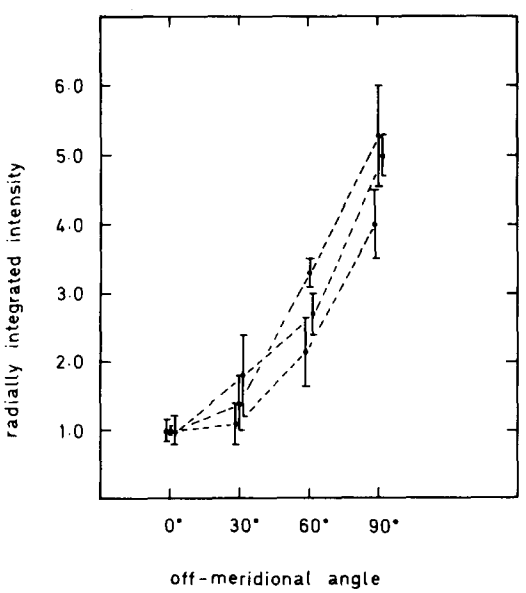

Fig. 4. Radially integrated intensity of the $(4.6\ \text{Å})^{-1}$ ring as a function of the angle from meridian to equator. Means and standard deviations of three independent experiments are given. See text for determination of baseline.

in the meridional densitometer trace. This baseline was then transferred onto the intermediate and equatorial traces by superimposing the peak maxima of the $(3.3\ \text{Å})^{-1}$ water band.

In exposures of the $(1.5\ \text{Å})^{-1}$ reflection with tilt angles $\phi \simeq 31°$, broad meridional diffraction maxima at about $(2.2\ \text{Å})^{-1}$ and $(1.2\ \text{Å})^{-1}$ were recorded also (Fig. 3). The proper tilt angles for these maxima are about 21° and 40°. A rough measure for the degree of disorientation of the membranes in the stack can be obtained from the arcing of the lamellar reflections (expressed as the angle α of the off-meridional spread of the reflections), if it is assumed that the structure of the pellet is cylindrically symmetric around the normal to the planes of the membranes; in good specimens $\alpha \simeq 15°$. Thus, even ideally meridional $(2.2\ \text{Å})^{-1}$ and $(1.2\ \text{Å})^{-1}$ reflections are allowed in exposures of 1.5-Å spacings with tilt angles $\phi = 31 \pm 5°$.

Discussion

Phytohemagglutinin M binds specifically to *N*-acetylgalactosamine residues or more complex glycopeptides [7,8]. The receptor site in the human erythrocyte is located in the oligosaccharide residues of glycophorin [9]; it is related to the membrane particles seen by freeze-etching [10]. The mean distance between receptors is about 200 Å in the human erythrocyte [11]. The sheep erythrocyte membrane is less well known, but similar receptor sites are assumed to be in human and sheep erythrocytes.

It is well established that the $(10.5\ \text{Å})^{-1}$ diffraction from biological membranes originates in membrane proteins [2,12]; it is never observed with pure membrane lipids, but is well explained as diffraction of α-helical or β-pleated sheet structures of membrane proteins [3,13]. A $(1.5\ \text{Å})^{-1}$ reflection from the repeat of amino acid residues is observed with α-helices [14]; in biological membranes it is taken as strong evidence for α-helical structures [3,15]. In conclusion, the equatorially accentuated $(10.5\ \text{Å})^{-1}$ diffration (Fig. 2) and the meridional $(1.5\ \text{Å})^{-1}$ reflection (Fig. 3) of the agglutinated ghost membranes are interpreted as diffraction from side-to-side packed α-helices whose axes are preferentially oriented perpendicular to the plane of the membranes. It is most likely that these α-helices belong to transmembrane proteins [16], although it can not be excluded entirely that oriented agglutinin molecules contribute to the $(10.5\ \text{Å})^{-1}$ diffraction. Meridional $(5.1\ \text{Å})^{-1}$ or off-meridional $(5.4\ \text{Å})^{-1}$ diffraction is not observed with the agglutinated membranes. Equatorial accentuation of the $(10.5\ \text{Å})^{-1}$ diffraction from erythrocyte membranes has not been reported previously [ref. 2, see also general discussion in ref. 3]. The degree of membrane disorientation in the specimens is not known accurately, but it can not be excluded that the agglutination results in structural reorganisations which involve transmembrane proteins and lipid phases of the membrane.

The $(4.6\ \text{Å})^{-1}$ diffraction (Fig. 4) is due to lipid phases in the membrane where the hydrocarbon chains are liquid-like and oriented perpendicular to the membrane [17,18]. Diffraction at $(2.2\ \text{Å})^{-1}$ and $(1.2\ \text{Å})^{-1}$ is not usually reported for biological membranes. The scattering curve of liquid normal tetradecane or pentadecane, however, has secondary maxima at those spacings [19] which are explained by the density distribution function in liquid long-

chain paraffins. In analogy, the (2.2 Å)$^{-1}$ and (1.2 Å)$^{-1}$ maxima (Fig. 3) are attributed to the lipid phase in the agglutinated membrane.

Time-dependent structural changes in the membrane specimens are a major obstacle for a quantative analysis. Changes in membrane structure are documented by the diffraction on the time scale of present exposure times (24—48 h). The equatorial (10.5 Å)$^{-1}$ diffraction is usually reduced or it may even disappear after about 72 h. Similar, but slower, changes are observed with the (4.6 Å)$^{-1}$ diffraction. After even longer periods lipid phase separations are recognised by characteristic diffraction patterns. The rate of specimens deterioration is not constant. A given specimen, especially with regard to lipid phase separation, may be well preserved for some time before it starts to degrade rapidly. All specimens which were kept for long time periods ultimately developed myelin figure-like structures. The data presented in Figs. 1—4 thus represent average images of slowly changing patterns. For this reason also the degree of equatorial accentuation of the (10.5 Å)$^{-1}$ diffraction (Fig. 2) must be considered a lower limit. However, gross perturbations such as loss of spectrin or intramembrane particle aggregation in fresh membrane specimens are excluded by gel electrophoresis and from freeze-etch electron microscopy. Serum albumin which is present in the specimens minimises vesicle formation and retards lipid phase separations, but it also interferes with the agglutination.

Acknowledgements

Freeze-etch electron microscopy was done by Dr. M. Müller of the ETH in Zürich. The excellent technical assistance of Miss H. Vortisch is gratefully acknowledged. Diffraction cameras were built by Mr. H. Müller of the Kantonsspital Basel. Financial support is by the Swiss National Science Foundation.

References

1 Lesslauer, W. (1976) Biochim. Biophys. Acta 436, 25—37
2 Finean, J.B., Coleman, R., Knutton, S., Limbrick, A.R. and Thompson, J.E. (1968) J. Gen. Physiol. 51, 19s—25s
3 Henderson, R. (1975) J. Mol. Biol. 93, 123—138
4 Loor, F., Forni, L. and Pernis, B. (1972) Eur. J. Immunol. 2, 203—212
5 Fowler, V. and Branton, D. (1977) Nature 268, 23—26
6 Maizel, J.V. (1971) in Methods in Virology (Maramorosch, K. and Koprowski, H., eds.), pp. 179—246, Academic Press, New York
7 Borberg, H., Woodruff, J., Hirschhorn, R., Gesner, B., Miescher, P. and Silber, R. (1966) Science 154, 1019—1020
8 Kornfeld, R. and Kornfeld, S. (1970) J. Biol. Chem. 245, 2536—2545
9 Marchesi, V.T., Tillack, T.W., Jackson, R.L. and Scott, R.E. (1972) Proc. Natl. Acad. Sci. U.S. 69, 1445—1449
10 Tillack, T.W., Scott, R.E. and Marchesi, V.T. (1972) J. Exp. Med. 135, 1209—1227
11 Elgsaeter, A. and Branton, D. (1974) J. Cell Biol. 63, 1018—1030
12 Blaurock, A.E. and Wilkins, M.H.F. (1969) Nature 223, 906—909
13 Pauling, L. and Corey, R.B. (1951) Proc. Natl. Acad. Sci. U.S. 37, 261—271
14 Perutz, M.F. (1951) Nature 167, 1053—1054
15 Blaurock, A.E. (1975) J. Mol. Biol. 93, 139—158
16 Bretscher, M.S. (1971) J. Mol. Biol. 59, 351—357
17 Luzzati, V. (1968) in Biological Membranes (Chapman, D., ed.), pp. 71—123, Academic Press, New York
18 Levine, Y.K. and Wilkins, M.H.F. (1971) Nat. New Biol. 230, 69—72
19 Stewart, G.W. (1928) Phys. Rev. 31, 174—179